Maria Sklodowska-Curie Actions (MSCA)
Innovative Training Networks (ITN)
H2020-MSCA-ITN-2018
Grant number 813137

Project number 813137

URBASIS-EU
New challenges for Urban Engineering Seismology

DELIVERABLE

Work Package: WP3
Number: D3.5 – Updated release of SPEED for city seismic response

Authors:	**Sangaraju, Srihari**	(POLIMI)
Co-authors:	Paolucci, Roberto	(POLIMI)
	Herlin, Aline	(formerly POLIMI)
Reviewer	Smerzini, Chiara	(POLIMI)

Approval	Management Board
Status	Final Version
Dissemination level	Public
Delivery deadline	31.10.2021
Submission date	31.10.2021
Intranet path	https://urbasis-eu.osug.fr/Scientific-Reports-157

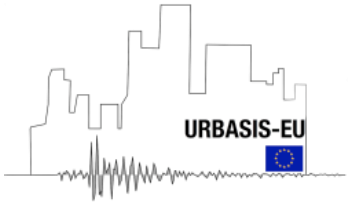

TABLE OF CONTENTS

1. Introduction 3
2. Overview of studies on Site-City Interaction (SCI) effects 5
3. Numerical algorithm to couple the ground motions with structural models at city-level 7
3.1 Geophysical modeling: Elastodynamic equation 8
3.2 Structural modeling: SDOF systems with and without SSI effects 9
3.3 Single lumped mass with a flexible soil-foundation system (4-DOF) 10
3.4 Coupling SDOF and 4-DOF systems in SPEED code 11
4. Results from validation test cases 14
4.1 Testcase 1: SDOF system with LE constitutive law 15
4.2 Testcase 2: SDOF with EPP constitutive law 15
4.3 Testcase 3: SDOF with Tri-linear constitutive law 17
4.4 Testcase 4: 4-DOF system 17
5. Conclusions and next developments 19
6. References 20
Appendix – User Guide 23

1. Introduction

In recent years, regional seismic hazard assessments are increasingly using 3D Physics-based simulations (PBS), as they are non-ergodic and provide region- and site-specific ground motions (GMs) with a realistic spatial correlation structure (Graves et al., 2011, p. 3; Bradley et al., 2020; Schiappapietra and Smerzini, 2021; Stupazzini et al., 2021). This growth in the use of PBS is mainly because of (i) a better understanding of earthquake sources, and the ability to synthetically generate rupture scenarios (Graves and Pitarka, 2016; Irikura and Miyake, 2011; Martin Mai and Beroza, 2003) (ii) mapping of sedimentary basins and growing database of 3D geological models (Small et al., 2017; Thomson et al., 2020., Koketsu et al., 2012) (iii) development of robust and efficient numerical tools based on accurate finite difference (FD), finite element (FE) and Spectral Element (SE) methods, in parallel with availability of computational resources (Komatitsch and Tromp, 2002; Mazzieri et al., 2013; Sjögreen and Petersson, 2012).

The accuracy of the PBS in the high-frequency range is generally bounded up to 1 – 3 Hz, owing, on the one hand, to the increased computational burden as the mesh gets finer to catch the shortest wavelengths propagating in soft soils, and, on the other hand, to the lack of detailed knowledge to construct a geological model with sufficient details also at short wavelengths. For this reason, very few simulations have reached maximum frequencies (F_{max}) of 10 Hz (Paolucci et al., 2021; Rodgers et al., 2020). Target F_{max} of PBS is crucial if the simulated ground motions are used in earthquake engineering applications, e.g. as input waveforms to study the dynamic response of structures.

For 3D earthquake simulations, it is common to impose absorbing boundary conditions on lateral and bottom surfaces to prevent the reflection of waves, the top surface is modelled as a traction-free surface to replicate ground surface and simulate free-field motions. In the presence of clusters of structures, the ground surface will be subjected to the application of significantly large inertial forces caused by the structural response. So, the traction-free condition may or may not be appropriate depending on the stiffness of the soil. If the local geology consists of soft sediments, this could modify the ground motion field (Gueguen, 2000; Wirgin and Bard, 1996). This phenomenon is referred to as Site-City Interactions (SCI).

Modelling buildings along with a geophysical model is a multi-scale problem, which demands huge computational resources, especially because target F_{max} should be high enough to capture structural vibration response. For this reason, fully coupled fault-to-structure simulations are very rare. However, in anticipation of future advancements in supercomputing, there is a need for computational tools which can generate GMs considering fully coupled simulations at an urban scale. This will be crucial to engineers and policymakers to directly evaluate the seismic demand of structures at an urban scale. In this regard, several workflows are being developed around the globe. Using SimCenter workflow, city-scale time history analysis is performed considering structures in San Francisco Bay Area (Lu et al., 2020), taking ground motions from the Cybershake experiment (Graves et al., 2011). Here, the structures are modelled using shear-deformation based tri-linear multi-degree-of-freedom systems, the hysteresis properties are obtained with minimal information like the number of floors, floor area, age etc. However, the structures are not coupled to PBS. To directly couple structural response with PBS, Taborda and Bielak (2011) has developed the Hercules framework, where PBS is first performed without considering small features like sediment basins and structures, then in the second stage, domain reduction method to apply the displacement fields calculated in the first step on to the smaller domain which consists of structures. This method is also being used in the EQSIM workflow (McCallen et al., 2021)

In the URBASIS project (ESR 3.4), we are developing the open-source, high-performance code SPEED available at http://speed.mox.polimi.it/ (Mazzieri et al., 2013), to couple the 3D physics-based regional

simulation of earthquake ground motion with the non-linear structural response. SPEED is based on spectral elements using Discontinuous Galerkin and can handle unstructured conforming and non-conforming meshes. This Deliverable aims at presenting the implementation and verification of a new module of SPEED, named SPEED-SCI, which allows to couple ground motion simulation with simplified models for linear and non-linear building response. Buildings can be modelled as a single degree of freedom (SDOF) or multiple-degree of freedom structures (MDOF), and coupling of ground response with the structural response is achieved by exchanging the interaction forces, like base reactions and moments, from structure to the ground surface at each time iteration. This module can be accessed from our git repository at https://bitbucket.org/ilmaz/speed.

SPEED-SCI module currently has the capability to model structure as (1) SDOF system with linear-elastic, elastic-perfectly plastic, tri-linear constitutive models. (2) 4-DOF system based on (Paolucci, 1997), to model soil-foundation-structure system and capture SSI effects. The implementations were verified using simple test cases, such as a single structure over rigid halfspace, and compared the structural response obtained from SPEED-SCI with numerical solutions from independent codes like OpenSees for the elasto-plastic SDOF system. Further, we plan to implement coupling of structures using MDOF model with nonlinear shear force-deformation relationships, and non-linear soil response based on Oral et al. (2017).

The report is organized as follows. Recent developments related to SCI effects and urban scale PBS are discussed in Section 2, and numerical approach for the solution of the elastodynamics problem along with the algorithm to couple response of structures with GMs are explained in Section 3. The validation test cases that were performed to test this module are reported in Section 4. Finally, the concluding remarks, along with planned future developments are discussed in Section 5 and the user manual for this module is attached as appendix.

2. Overview of studies on Site-City Interaction (SCI) effects

The standard ground motion simulations consider wave propagation accounting for site effects including (i) amplification of ground motions in superficial soft sediments considering nonlinearity, basin-shape effects, heterogeneity of velocities within the basin, and (ii) focusing and scattering of wave fields due to topography. But in addition to site effects, densely packed buildings in urban areas can produce modifications of the wave fields because of the SCI effect.

One of the first experiments to study SCI using a real building was performed by Jennings (1970), where the ground motions induced from vibration tests of a library building were recorded up to a few kilometres of radius in the surroundings, due to the presence of soft sediments. Similar resonance effects are commonly observed, especially during rock concerts, where the synchronised movement of the audience induced severe vibrations and lead to damage of structure (Erlingsson and Bodare, 1996). Even though these examples are just based on vibrations caused by a single structure, these findings give an idea about, how the earthquake ground motion can get modified. In presence of a group of buildings, like a city, SCI effects can either downplay ground motions or even enhance them. For example, one of the reasons for the large amplifications corresponding to long periods of ground motions during the 1985 Mexico earthquake, is also attributed to seismic waves being trapped in soft soil, as densely packed structures diffracted back them back into the soil (Wirgin and Bard, 1996). Gueguen et al., (2002) accounted for the SCI effects on free-field ground motion and attempted to simulate ground motion using a recorded ground motion at a reference site during the 1985 Mexico earthquake.

In an ambient-noise response experiment of a building in Lyon, France, the difference in building response in presence and after the demolition of 2 other structures in close vicinity is noted (Hans et al., 2005), which suggests dynamic interaction between different structures through the soil. Dynamic soil response in urban areas is theoretically modelled and validating against shake table experiments, considering the soil which is reinforced with piles (Boutin et al., 2014).

Several attempts have been made to numerically model SCI effects, like modelling different building configurations and subjecting them to plane wave excitation (Kham et al., 2006; Semblat et al., 2008). Small scale experiments with shake tables subjected to plane waves are performed to validate SCI effects modelled using numerical methods (Schwan et al., 2016). The structures here are designed on small scale, as identical resonator structures at arraigned at regular spacing lying on top of an idealised soil column. Figure 1 shows the response recorded at top of the soil layer when subjected to a richer wavelet excitation at bottom of the soil layer. The recorded acceleration at top of the soil in presence of just 37 resonators changed significantly compared to the presence of just 1 resonator.

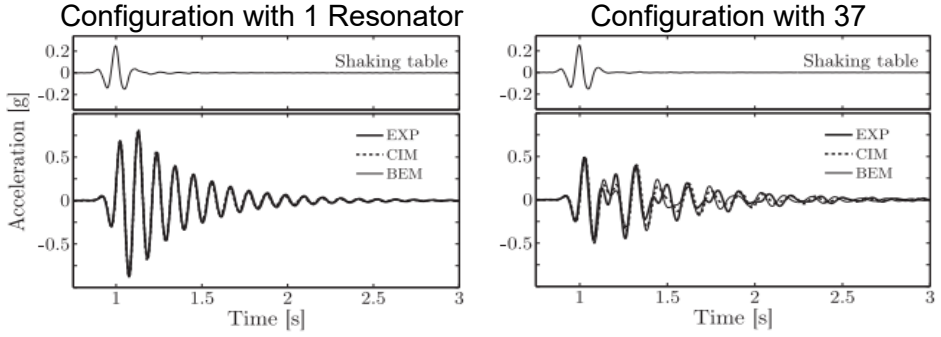

Figure 1 Comparison of acceleration time histories from shaking table experiments with results from numerical simulations (Schwan et al., 2016).

To investigate SCI effects using more sophisticated structural models, Lu et al., (2018) have modelled the buildings as MDOF and coupled them with wave propagation simulations. Clusters of buildings are considered on top of a hypothetical trapezoidal basin subjected to plane waves, to explore the extent of change in peak ground acceleration values considering SCI effects.

Few attempts are also made to simulate multi-scale PBS, where the structural response is coupled with ground motions. 3D physics-based simulations of the 2011 Christchurch earthquake are performed using SPEED code, with structures being modelled as elastic bricks on top of free-surface as shown in Figure 2 (Guidotti et al., 2011). Taking advantage of the domain reduction method in Hercules code (Taborda and Bielak, 2011), ground motions from PBS during the Northridge earthquake are coupled with the structures considering the region of San Fernando Valley (Isbiliroglu et al., 2015). Targeting to simulate high-frequency ground motions (~11Hz), Zhang et al., (2021) has simulated PBS considering the Istanbul region, where rupture, wave propagation, soil response and the structural response are simulated separately, but coupled with each other using the domain reduction method. Also aiming at high-frequency simulations with coupling, McCallen et al., (2021) have devised 'EQSIM' workflow, which is again a two-stage process based on domain reduction method. In this workflow, the stochastic perturbations are also added to the available 3D geological model, to improve the resolution, thereby improving the quality of the high-frequency content of ground motions.

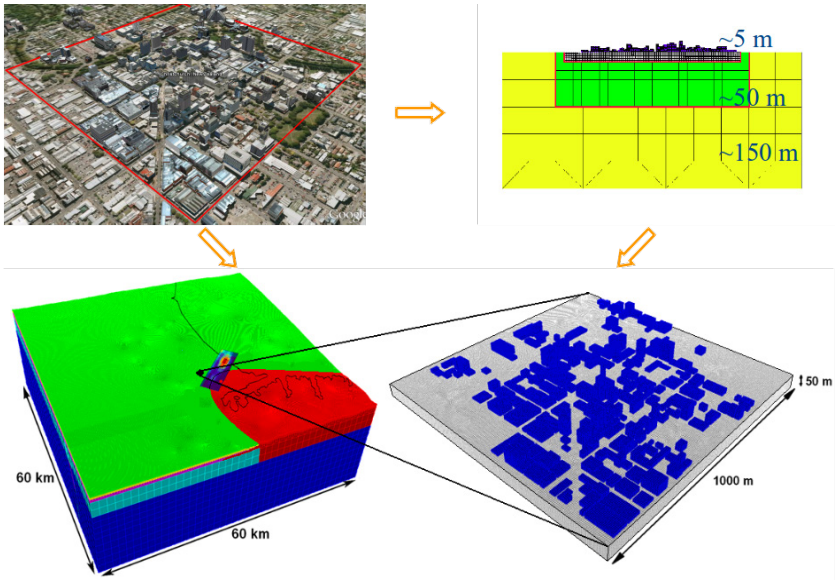

Figure 2 Modelling of structures as elastic blocks in a Multi-scale earthquake simulation of The 2011 Christchurch Earthquake (Guidotti et al., 2012)

3. Numerical algorithm to couple the ground motions with structural models at city-level

The generation of seismic damage scenarios in large urban areas represents a key tool for civil protection to enhance earthquake preparedness, to establish effective prevention policies for seismic risk mitigation and to support decision making in emergency management. Usually, such scenarios are produced using approaches based on segregated algorithms, where the simulation of the ground response is decoupled from that of the buildings so that the dynamic interaction forces exchanged by the soil and the structure are not taken into account. However, the scientific and technological advances made in recent years have given rise to increasingly flexible, accurate, and scalable numerical methods, and have opened up new perspectives in the numerical modelling of multi-scale seismic phenomena including, in a single model, the seismic source, the propagation in heterogeneous materials, and the dynamic response of civil engineering structures. This integrated approach makes it possible to perform three-dimensional physics-based simulations of seismic risk scenarios at the urban scale, taking into account soil-structure interaction (SSI) and site-city interaction (SCI) effects.

To achieve this goal, we have enhanced the code SPEED by implementing a new module (SPEED-SCI) suitable to couple regional ground motion simulations with simplified models for non-linear structural response at an urban scale. The conceptual framework behind the "source-to-structure" approach for seismic wave propagation simulation is sketched in Figure 3. The structures are often modelled as lumped mass systems. For both simplicity and computational efficiency, we model the buildings with help of lumped mass systems. In this current version of code, structures can be approximated as single mass systems with (i) fixed-base (SDOF) or (ii) flexible base foundation to study soil-structure interaction (4-DOF)

In this section, the elastodynamic equation and numerical modelling of PBS are briefly outlined, before going into details about the structural models currently available in SPEED-SCI and the algorithm for coupling ground and structural response.

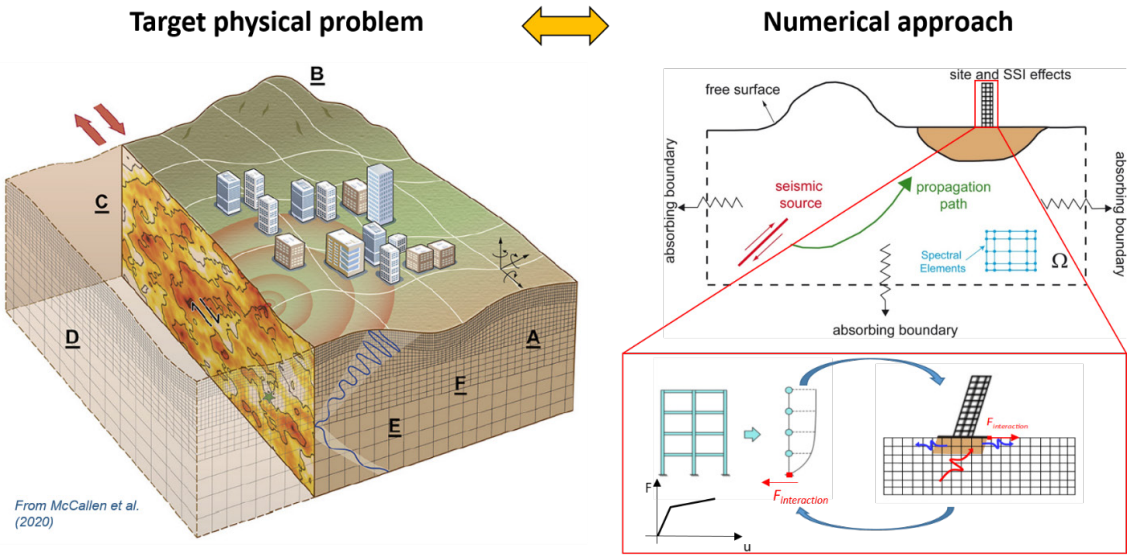

Figure 3 Framework for coupling wave propagation from source-to-structure.

3.1 Geophysical modeling: Elastodynamic equation

In PBS, we consider the earth's crust as a continuum body (Ω) and model it is using realistic geology. Let $\partial\Omega$ be the external boundary, and ∂S be the internal discontinuity or fault plane inside the domain Ω. At any given point inside Ω , having the mass density of ρ and corresponding body forces b, the principle of conservation of linear momentum is given by Equation 1, which is also known as the elastodynamic equation. Here, u is displacement and σ is Cauchy stress tensor. We consider the medium as visco-elastic material, to provide damping which facilitates the anelastic attenuation of seismic waves. Then the dynamic equilibrium equation will be Equation 2, where ξ is the damping term derived from quality factors (Q).

$$div\,\boldsymbol{\sigma} + \boldsymbol{b} = \rho\ddot{\boldsymbol{u}} \tag{1}$$

$$div\,\boldsymbol{\sigma} + \boldsymbol{b} = \rho\ddot{\boldsymbol{u}} + \{\, 2\rho\xi\dot{\boldsymbol{u}} + \rho\xi^2\boldsymbol{u} \,\} \tag{2}$$

Among various numerical techniques available to solve Equation 2, the finite difference (FD) and the finite element (FE) methods proved to be more practical. The high-performance code SPEED is based on Spectral Element Method (SEM), which is based on higher-order FE, and computationally efficient to solve problems related to wave propagation, acoustics, and fluid mechanics. The SEM is accurate even when the mesh contains distorted elements (Komatitsch and Vilotte, 1998; Oliveira and Seriani, 2011). This is a huge advantage in earthquake simulations, as they involve complex geometries like fault planes and other geological interfaces.

The stress tensor can be related to the displacement field with help of constitutive laws and compatibility equations. Further, the weak form of Equation 2 can be discretized, giving way to Equation 3 which is in matrix form. With the use of Gauss–Lobatto-Legendre (GLL) quadrature points, mass matrix (M) will be diagonal which saves computational time. Here C, K and C represent damping, stiffness, and force matrices respectively. Time integration is performed using the Leap-Frog method.

$$M\ddot{\boldsymbol{u}} + C\dot{\boldsymbol{u}} + K\boldsymbol{u} = F \tag{3}$$

The earthquake source can be modelled (i) using spontaneous dynamic rupture propagation on ∂S, for which one needs to define stress conditions and friction laws, (ii) using kinematic rupture source, where we directly consider slip-on fault plane as input. In kinematic rupture source, the fault plane is discretized into small patches and each patch is assumed as a double couple point source. SPEED code supports both source assumptions, the kinematic model implementation has been validated extensively (Paolucci et al., 2015; Smerzini et al., 2017; Sangaraju et al., 2021).

In addition to the earthquake source inside the domain, the external boundaries ($\partial\Omega$) can also be constrained using a variety of boundary conditions, like displacement constrained Dirichlet condition, force constrained Neumann condition, Stacy's absorbing boundary conditions. Using these conditions, one can use SPEED to solve a diverse range of problems involving elastic wave propagation.

3.2 Structural modeling: SDOF systems with and without SSI effects

Consider a single mass (m) that is supported on top of a massless column with lateral stiffness (k). Neglecting small axial deformations, the mass can move only in lateral directions. We further assume that lateral motion is decoupled, meaning that the response of the system can be obtained by solving a single equation. These systems are referred to as the single degree of freedom systems (SDOF). It should be noted that the base of the system is assumed to be fixed, restricting any possibility of rotations and relative displacements between soil and foundation. The structures dissipate some energy during motion because of internal material friction, formation of microcracks etc. So, we can further add a dash-pot damper to the system as shown in Figure 4. The term c represents the damping coefficient of structure, which can be derived from damping ratio ξ.

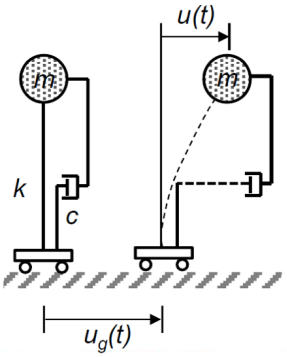

Figure 4 SDOF system under a ground excitation.

During an earthquake, let the displacement of ground motion below the structure be u_g. The base will move along with the ground, however inertial forces ($m\ddot{u}_g$) act on lumped mass to resist the along with the base. This relative displacement (u_{sys}) between the base of the structure and lumped mass will cause the development of the lateral restoring force (F_s) in the column, and a damping force (F_c). If stiffness of the structure is too high, then u_{sys} will tend to zero. If stiffness is too low, the mass will tend to stay at rest in its original position and u_{sys} will be maximum. The total acceleration of the system ($\ddot{u}_t$) is the sum of ground acceleration and relative acceleration of lumped mass ($\ddot{u}_g + \ddot{u}_{sys}$), then equilibrium equation of structure can be written as Equation 4.

$$m\ddot{u}_{sys} + F_c(\dot{u}_{sys}) + F_s(u_{sys}) = -m\ddot{u}_g \tag{4}$$

This equation is in a generalized form and applies even to both linear and nonlinear SDOF systems by modifying the $F_s(u_{sys})$ term accordingly. In current version of SPEED-SCI module, the SDOF systems can be used along with following lateral force (F_s) – displacement (u_{sys}) relationships:

(1) Linear-Elastic (LE) - The stiffness k of the structure remains constant, independent F_s.

(2) Elastic Perfectly Plastic (EPP) - The structure will behave linearly with stiffness k, when F_s is less than yield strength (f_y). Above this threshold, the system will have no stiffness and undergoes permanent deformation.

(3) Tri-linear – The force-displacement relation is defined based on three limit state values as shown in Figure 5. These limit states are usually referred as, linear-elastic, strain-hardening zone where non-linear behavior of structure will start and structure may reach maximum possible strength (f_y), strain-softening zone where structural strength further deteriorates.

Several techniques are also present to idealise multi-story buildings as Multiple Degrees of Freedom (MDOF) systems based on tri-linear shear force and deformation relations (Lu et al., 2020). In this version of code, we limit to SDOF but in future developments, we plan to develop a more sophisticated structural model like the MDOF shear model.

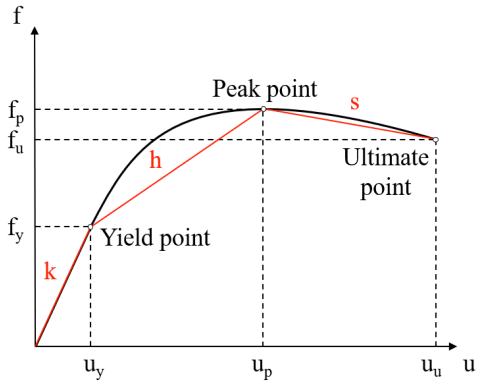

Figure 5 Tri-linear approximation (red) of the structural capacity

3.3 Single lumped mass with a flexible soil-foundation system (4-DOF)

In SDOF systems, we assume the base to be fixed. This assumption is good enough when a structure is on top of a stiff rock. When the foundation of the structure is laid on soft sediments, there will be relative displacements between ground and foundation of structure along with the rotation of structure, creating soil-structure interaction (SSI). Figure 6a shows the soil-foundation-structure system. The motion at the ground surface u_g will cause a motion u_f on foundation after SSI, which will in turn cause motion u_s on lumped mass of structure. The soil-structure interaction can be seen as a superposition of two phenomena (Wolf, 1985) (i) Kinematic Interactions, where foundation and structure are assumed as massless, and foundation will act as diffraction source as the stiffness of soil and foundation are different. (ii) Inertial Interaction is caused by the action of inertial forces of structure on the soil.

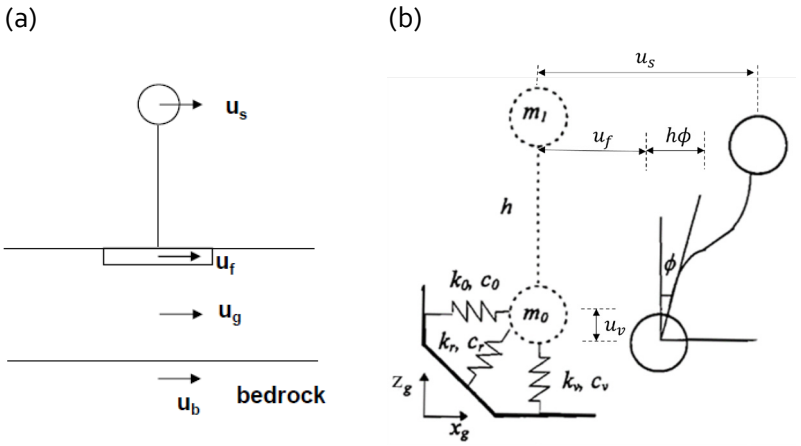

Figure 6 (a) Soil-foundation-structure system (b) 4-DOF model of the soil-foundation-structure system (Paolucci 1997)

Following Paolucci, 1997 we model the soil-foundation-structure system using 4 degrees of freedom (4-DOF). Under specific assumptions like the vertical incidence of seismic waves, the kinematic interaction will have negligible effects (Wolf, 1985). In this work, the contribution only from the inertial interaction is considered. These 4 DOF's are the (i)Lateral movement of lumped mass relative to ground (u_s), (ii)Lateral movement of foundation with respect to ground (u_f), (iii) Rotation at foundation caused by lateral

movement of lumped mass (ϕ), (iv)Vertical displacement of foundation (u_v) (Figure 6b). One can neglect also neglect the vertical displacement at foundation, to further simplify the model.

Now we have both lumped mass of structure (m_1) and mass of foundation (m_0). Considering a linear-elastic behavior, the lateral stiffness k_o, vertical stiffness k_v, similarly damping coefficient in the lateral direction is c_o and vertical direction is c_v can be obtained by evaluating dynamic impedance matrix (Gazetas, 1991). The rotation at the foundation will allow us to consider the flexibility of the foundation-structure system, the moment reaction (M) is given as $k_r\phi$ which is also linear-elastic, k_r is rotational stiffness, c_r is damping corresponding to rotation. The force-displacement relation of the lumped mass structure is linear-elastic and given by lateral stiffness k_1 , and damping coefficient c_1.

Considering the displacement matrix of the 4-DOF system as $x = [u_s, u_f, \phi, u_v]^T$, we can write the equilibrium equations of the decoupled system as shown in Equation 6. Here, M is the diagonal mass matrix, C is assembled damping matrix, K^S is assembled stiffness matrix which depends on The force-displacement relation of the lumped mass structure is linearly elastic and given by lateral stiffness k_1 , and damping coefficient k_1 (Herlin., 2021). F and P are the force vectors related to reaction forces at the foundation and inertial forces developed in the directions of individual DOFs.

$$M\ddot{x} + C\dot{x} + K^S x + F = P \tag{6}$$

3.4 Coupling SDOF and 4-DOF systems in SPEED code

When a structure is subject to ground shaking, it will in turn transfer the inertial forces and moments back onto the ground surface (Figure 7). The new SPEED-SCI module is designed to achieve the same task i.e., transferring forces from the ground surface to simplified structural models (SDOF and 4-DOF) and vice-versa at each time step to achieve the coupling, while at the same time not spending any additional computational resources. The computational time of 3D Physics-Based Simulation (PBS) with and without structures is almost the same.

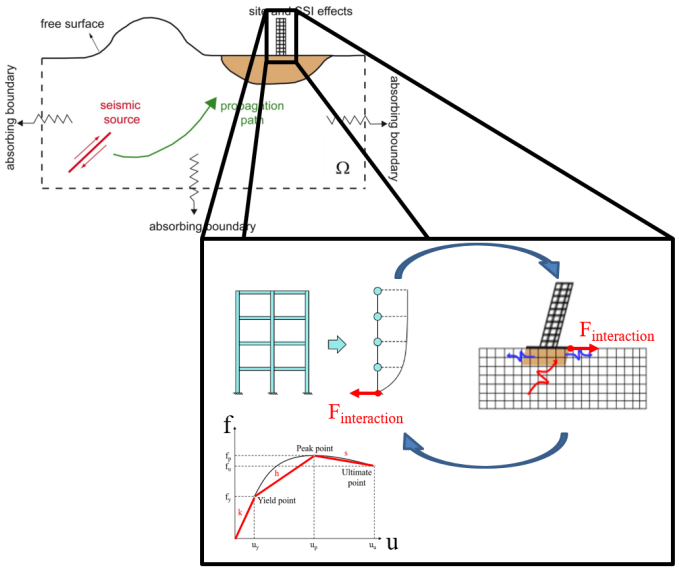

Figure 7 Exchange of interaction forces between ground surface and simplified structural system

Now that we have seen both elastodynamic equation (Equation 3) and equations of motion governing SDOF (Equation 4) and 4-DOF system (Equation 6), the algorithm we used for coupling of the response of ground and structure at each time step is discussed here.

Consider that while solving Equation 3 in the time domain, the time discretization used is Δt, such that at n^{th} time step, time t^n is $n\Delta t$, and the displacement at a point on the ground surface is ${u_g}^n$. In the n^{th} time step, we compute the ground displacement ${u_g}^{n+1}$, from ${u_g}^n$ and ${F_{PBS}}^n$ (Mazzieri et al., 2013). The force vector ${F_{PBS}}^n$ in will also have contribution from reaction forces ${F_{sys}}^n$ caused by structural systems. For example, to calculate solution at time t^1 (i.e., 0^{th} time step) we will need initial values ${u_g}^0$, ${\dot{u}_g}^0$, ${F_{sys}}^0$, ${F_{PBS}}^0$ at time $t^0 = 0$, which are usually set to be zero.

Before marching into $n + 1^{th}$ time step, we need to calculate ${F_{sys}}^{n+1}$. Steps involving the calculation of ${F_{sys}}^{n+1}$ are shown in the schematic diagram (Figure 8), and the implementation of the SDOF system using the LE model is explained below:

(i) Using central difference scheme, ground acceleration at n^{th} time step (${\ddot{u}_g}^n$) can be approximated as shown in Equation 7 and applied to the structural system.

$$ {\ddot{u}_g}^n = \frac{{u_g}^{n+1} - 2{u_g}^n + {u_g}^{n-1}}{\Delta t^2} \tag{7} $$

(ii). Again, using central difference scheme to approximate time derivatives of ${u_{sys}}^n$ we can get equations of motion in algebraic form (Equation 8) and calculate the only unknown ${u_{sys}}^{n+1}$.

$$ m * \frac{{u_{sys}}^{n+1} - 2{u_{sys}}^n + {u_{sys}}^{n-1}}{\Delta t^2} + c\frac{{u_{sys}}^{n+1} - {u_{sys}}^{n-1}}{2*\Delta t} + k{u_{sys}}^n = -m{\ddot{u}_g}^n \tag{8} $$

(iii) In the final step, we calculate base reactions ${F_{sys}}^{n+1}$ (Equation 9) and sum it to ${F_{PBS}}^{n+1}$.

$$ {F_{sys}}^{n+1} = k * {u_{sys}}^{n+1} \tag{9} $$

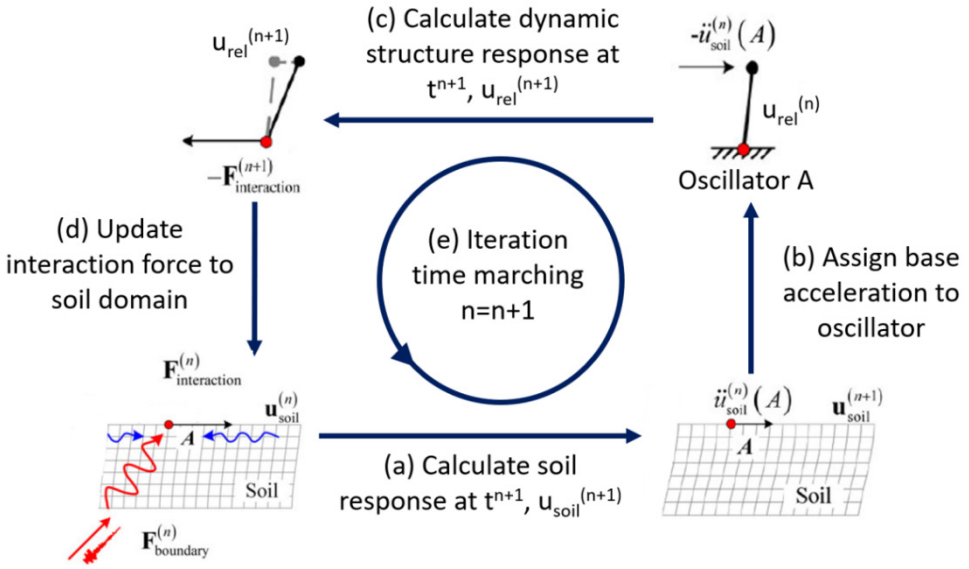

Figure 8 Schematic diagram showing coupling of ground motion and structural response at each time step

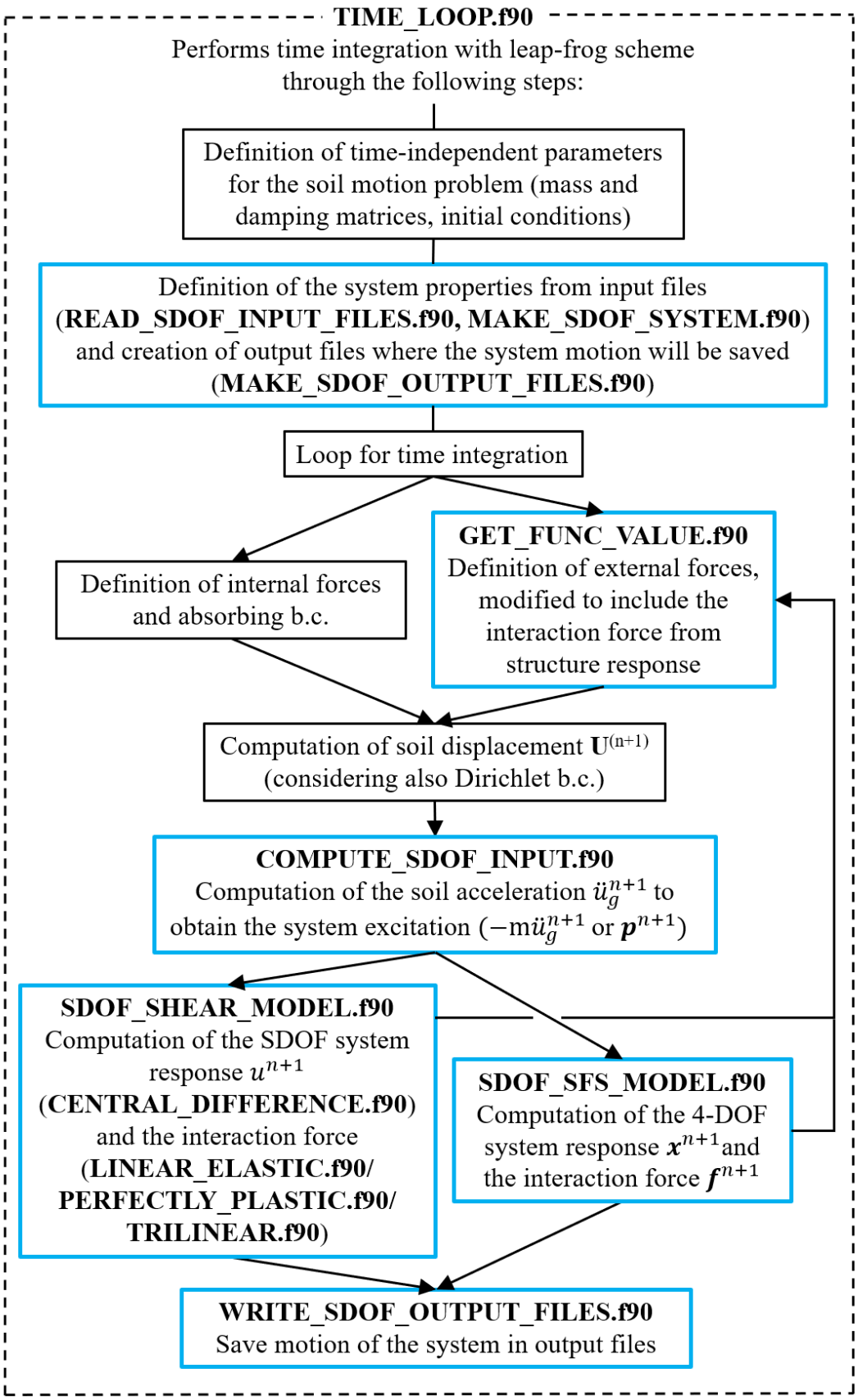

Figure 9 Schematic Flowchart of the newly implemented SPEED-SCI module.

.

4. Results from validation test cases

Some preliminary test cases have been simulated using the newly implemented SPEED-SCI module. Using these test cases, we have validated the accuracy of SDOF with the above discussed constitutive models, and the 4-DOF system. In this section, first, the problem description of test cases using only one structure on top of half-space are explained, along with results. Only a few test cases that were simulated are reported here, we refer to Herlin. (2021), for further details.

A homogeneous rigid half-space of dimensions 10km*10km*5.5km is modelled as the simulation domain (Figure 10). The medium has a density of 2500 kg/m^3 with shear wave velocity (V_s) of 2000 m/s and pressure wave velocity (V_p) of 4000 m/s. Frequency-dependent damping is assumed, with quality factor (Q) set as 100. The domain is subjected to a plane wave excitation in the x-direction applied at the bottom surface. The plane wave excitation is a Ricker wavelet in the time-domain with a maximum displacement of 1 cm, having peak frequency (f_{peak}) of 1 Hz and maximum frequency (f_{max}) of 3 Hz (Figure 10.b). The domain is discretized using a mesh with an element size of 500m, and a spectral degree of 4, so that, the generated ground motions are accurate till 4 Hz.

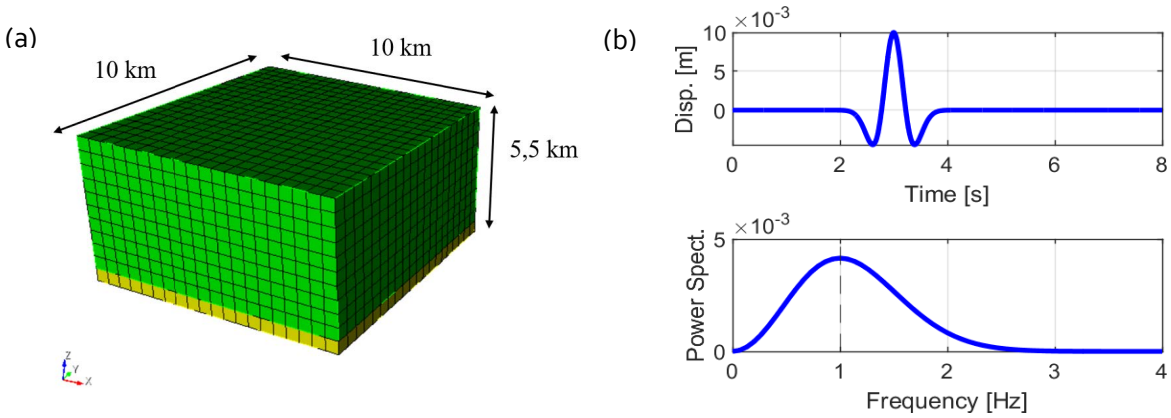

Figure 10 (a) Domain consisting of homogeneous half space. (b) Ricker wavelet used as plane wave excitation

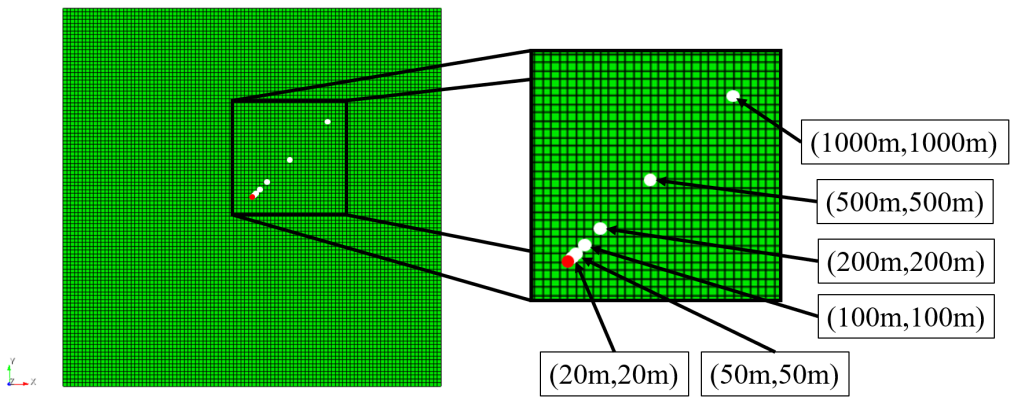

Figure 11 Top surface of the domain. Red dot represents centroid of the surface, where the structure is placed. White dots are additional points selected to monitor the ground motions.

Lateral boundaries of the domain are constrained to have zero displacements in Y and Z directions, and the bottom surface is modelled as an absorbing boundary. Free-surface condition is applied on the top surface,

but a single structural system is assumed at the centroid of the surface as shown in Figure 11. Few other points are selected in the neighborhood of the structure, to monitor any change in ground motion, because of the presence of structure.

We have tested four different cases: SDOF system with three different constitutive models and 4-DOF system. In some test cases, few trial simulations were performed, by varying structural properties like yield strength (f_y), to explore different possibilities. Of course, the fundamental structural frequency ($\omega_n = 1/T_n$), should be lower than the frequency limit of the numerical model . Here, the modelled mesh is capable of simulations up to 4Hz, so the structural response above 4Hz may not be reliable.

4.1 Testcase 1: SDOF system with LE constitutive law

In this test case, we model the SDOF system considering LE behaviour. Two different structures are assumed with T_n of 1 sec, so than the corresponding fundamental frequency ω_n is 1sec. Accordingly, the m and k of the system are set as 50 $tons$ and 1970 KN/m respectively. The damping ratio (ξ) is assumed as 5%. The displacement response of the structure u_{sys} calculated using the SPEED-SCI module is compared with the numerical solution calculated using OpenSees code (Figure 12. a). The solution calculated using both codes is identical. The dynamic amplification factor (D) of structural response from SPEED-SCI coincides with the theoretical solution (Figure 12. b), the maximum value of D is given as $1/2\xi$, equal to value of 10 for the considered structure. For this test case, since only one structure is considered, the modification of ground motion nearby the structure is not observed.

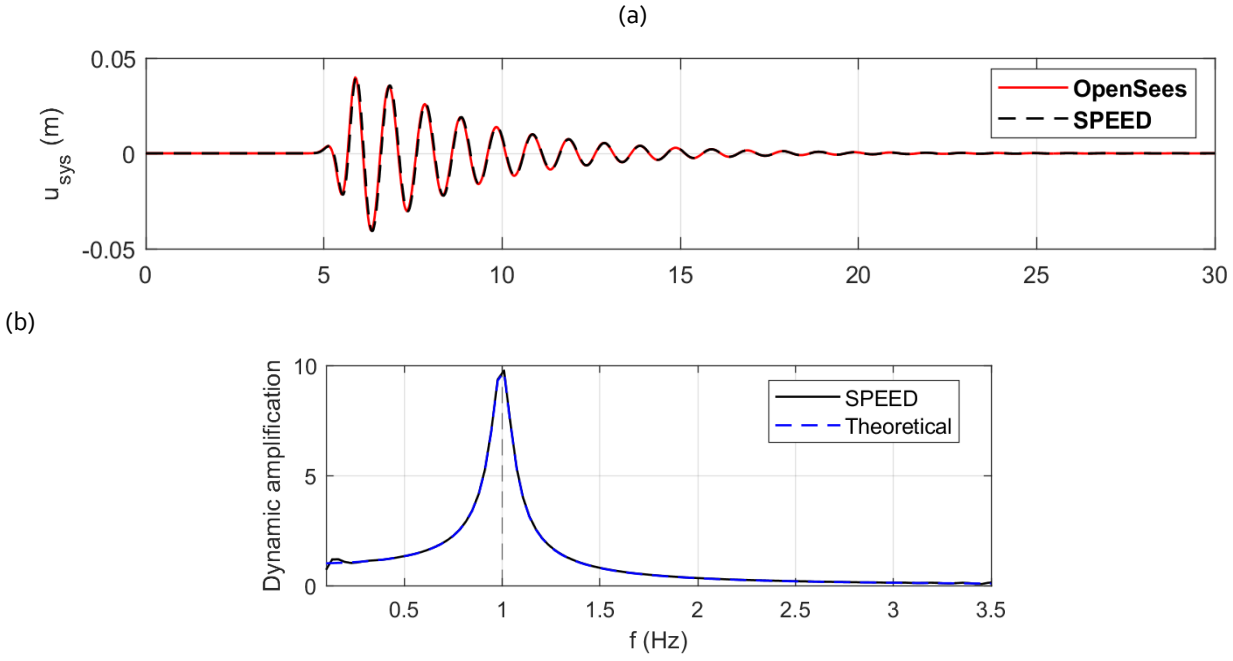

Figure 12 SDOF with LE (a) Comparision of displacement time histories calculated using SPEED and OpenSees (b) Dynamic amplification factor

4.2 Testcase 2: SDOF with EPP constitutive law

Let the maximum forces developed in a structure because of an excitation considering LE and EPP systems be f_o and f_{EPP} respectively. The ratio and f_{EPP}/f_o is defined as yield strength reduction factor (R_y), which can always be greater than or equal to 1, R_y = 1 means that the structure with EPP behaviour is still in the

elastic regime. In this test case, we consider the same structural parameters that were used in the LE test case, but we change the value of yield strength f_y.

Table 1 Maximum structural displacement (u_m) and permanent displacment (u_{perm}) using SPEED (SP) and OpenSees (OS)

R_y	f_y		u_m [m]	u_{perm} [m]
0.9953	81	SP	0.041	0
		OS	0.040	0
2.0155	40	SP	0.042	0.021
		OS	0.042	0.021
4.0311	20	SP	0.025	0.008
		OS	0.024	0.008
8.0622	10	SP	0.029	0.006
		OS	0.028	0.006

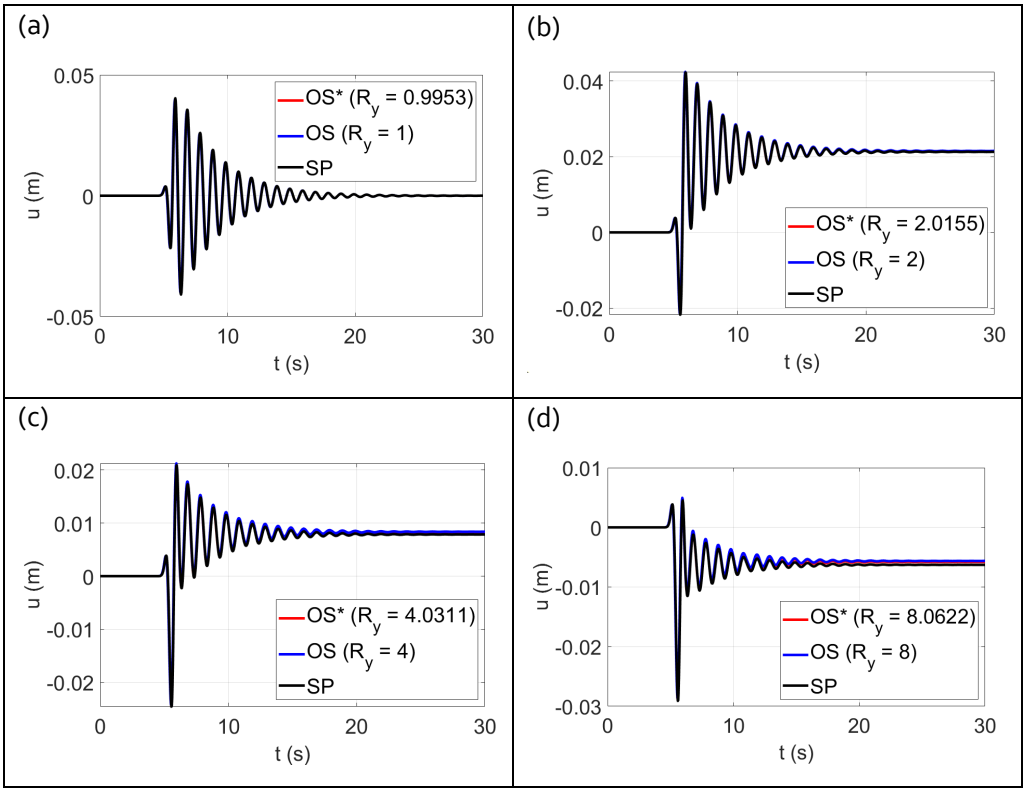

Figure 13 Comparision of displacement time histories calculated using SPEED (SP), and OpenSees (OS) for (a) $R_y = 1$ (b) $R_y = 2$ (c) $R_y = 3$ (d) $R_y = 4$

Four different simulations are performed, such that system will have $R_y = 1,2,4,8$ respectively. In the LE test case, maximum structural displacement (u_m) is 0.041 m corresponding maximum force ($f_o = k * u_m$) is 80.6 KN. The permanent displacement at the end of excitation (u_{perm}) and maximum displacement u_m and are computed using both SPEED-SCI and OpenSees codes. The percentage difference in values from

both methods are less than 1.5% (Table 1). The displacement time histories calculated using both codes are comparable in all 4 simulations. (Figure 13).

4.3 Testcase 3: SDOF with Tri-linear constitutive law

In this test case, a tri-linear constitutive law is used. We start with the same basic structural parameters m, k and ξ that were used in the LE test case. Further, the stiffness corresponding to strain hardening zone h is assumed as $0.2k$. For simplicity, we have modelled this test case such that the structure will not reach peak point (Figure 5), however, the test cases considering tri-linearity are explained in Herlin., (2021). Once we estimate force at yield point (f_y) and peak point (f_{peak}), we can evaluate displacemnets corresponding to these limit states from k, h. Here we considered f_y as 40KN, corresponding to R_y of 2, and a very large value is used as f_{peak}, to avoid strain-softening. The structural displacements calculated using SPEED-SCI are again in agreement with the solution from OpenSees (Figure 14. a). Figure 14. b shows corresponding hysteresis behaviour captured in the SPEED simulation, along with the constitutive law that has been assumed for this test case.

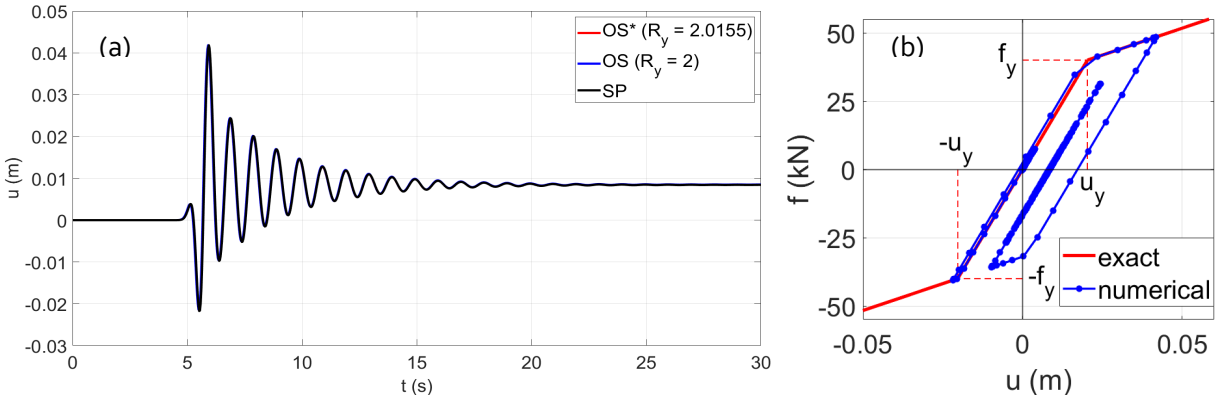

Figure 14 SDOF-Trilinear test case. (a) Comparision of Structural displacements from SPEED and OpenSees codes. (b) Hysteresis behaviour of structure from SPEED simulation.

4.4 Testcase 4: 4-DOF system

The 4-DOF implementation of structure gives us the flexibility to consider foundation-structure interaction, along with the capability to capture SSI, while using a simple model. In this test case, we also have to consider the mass of the foundation and parameters describing soil-structure interaction. To be consistent with previous test cases, mass, lateral stiffness, damping related to lumped mass are kept the same. With reference notation in section 3.3, the details of input parameters for this test case are presented in Table 2.

In this simulation, we are solving for 4 degrees of freedom: (i) Total lateral displacement of the structural mass relative to the ground u_s, (ii) Lateral displacement of foundation relative to the ground u_f, (iii) The angle of rotation/deflection of the structure near the foundation ϕ, (iv) Vertical displacement u_v. Owing to the large stiffness in the vertical direction, and since the plane wave is applied only in the lateral direction, the vertical displacements coming out of simulation are negligible. We can describe u_s as summation of u_f, $\phi * h$, $u_{s,f}$, where $u_{s,f}$ is the contribution made by the structure's lateral stiffness to the relative displacement between the structural mass and the foundation. Figure 15 shows the time-history plot of $u_{s,f}$, u_f and ϕ, calculated from SPEED-SCI. These results are compared with Matlab routines developed following the procedure of Paolucci., (1997). Two numerical solutions are identical again, proving the accuracy of the

SPEED-SCI module. In **Error! Reference source not found.**, the $u_{s,f}$ from 4-DOF test case is compared with structural displacement obtained using SDOF- LE test case. The displacement oscillations of $u_{s,f}$ has longer periods compared to the SDOF case, suggesting that the T_N of the structure has been increased because of SSI effects considered in the model. The T_N, is essentially casued by the decrease in lateral stiffness between lumped mass and foundation, as the foundation is flexible in 4-DOF and fixed in the case of SDOF.

Table 2 Input parameters: the 4-DOF test case

$m_1\ [ton]$	50	$k_0\ [KN/m]$	500000
$k_1\ [KN/m]$	1970	$c_o\ [tons.s/m]$	1000
$T_N\ [s]$	1	$k_v\ [KN/m]$	1500000
$m_o\ [ton]$	10	$c_v\ [tons.s/m]$	15000
$J\ [ton.m^2]$	48	$k_r\ [KN.m/rad]$	5500000
$h\ [m]$	10.8	$c_r\ [KN.m.s]$	3000

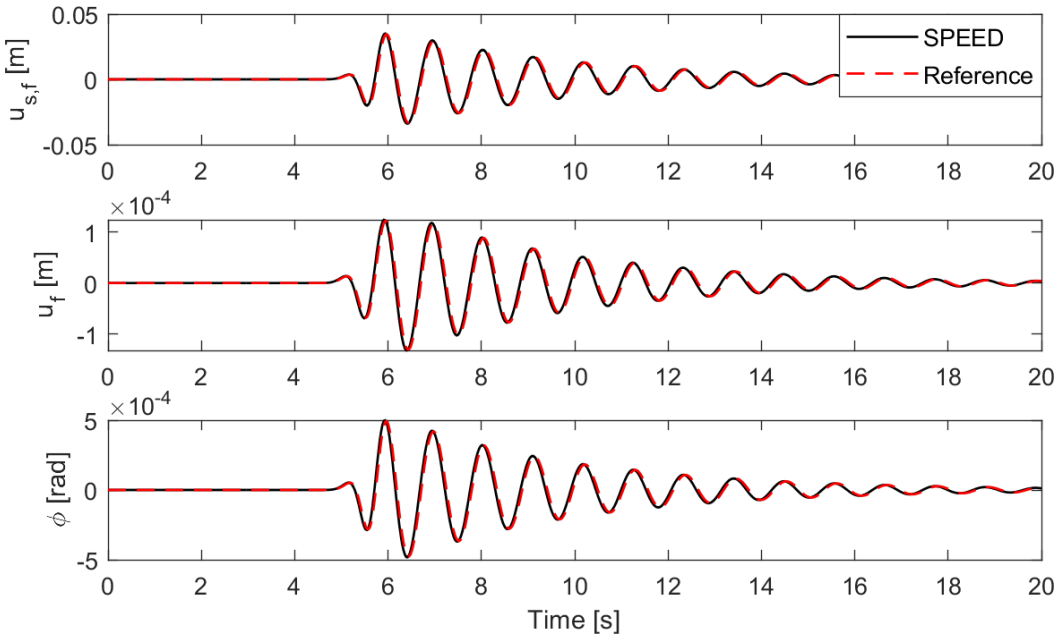

Figure 15 4-DOF testcase. Comparison of different degrees of freedom, calculated using SPEED, and reference solution from Matlab routines

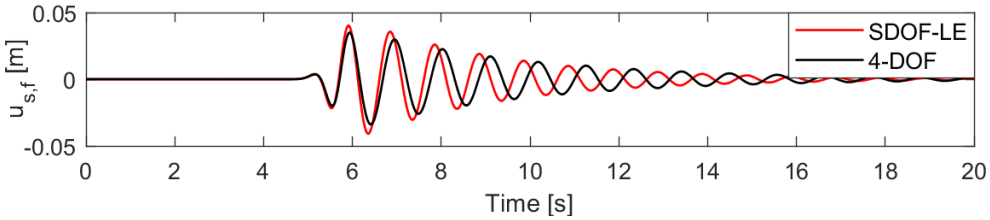

Figure 16 Comparison of lateral displacement of structure from SDOF-LE and 4-DOF testcases

5. Conclusions and next developments

It is known that local site and site-city interaction (SCI) effects can modify the ground motion field in terms of amplitude, frequency content and spatial variability features. Physics-based numerical simulations accounting for the coupled wave propagation from the fault rupture to structures are multi-scale in nature, and, therefore, require significant computational resources. To address this multi-scale PBS, we have implemented a new module (SPEED-SCI) in the high-performance code SPEED (http://speed.mox.polimi.it/) to couple physics-based ground motion simulations with reduced models for both linear and non-linear structural response.

The main features of the numerical approach can be summarized as follows:

- The numerical paradigm is suitable for multi-scale seismic wave propagation from the seismic source, to the ground surface, up to the interaction with the non-linear response of clusters of buildings in urbanized environments;
- The coupling algorithm is embedded in the SPEED kernel at each time step, making it computationally efficient;
- The structural response is modelled using linear and non-linear SDOF or MDOF models;
- Clustered SDOF/MDOF models are handled to catch the building-soil-building interaction effects;
- Soil-structure interaction (SSI) and site-city interaction (SCI) effects are accounted for.

In this module, simplified structural models, as SDOF/MDOF systems, are accounted for, and, at each time iteration of the PBS, the interaction forces are calculated and exchanged between the structure and the ground. Although the approach is simplified in terms of structural modelling, the main advantage lies in the limited modelling and computational cost, because (i) the mesh does not have to include the comparatively small structures on top of a large-scale geological domain and (ii) the computational time of the simulation with and without structures is almost same.

In this current version of SPEED-SCI, structures can be modelled as SDOF system with (i) Linear-elastic (ii) Elastic perfectly plastic, (iii) Tri-Linear constitutive laws and (iv) 4-DOF system representing soil-foundation-structure, to include SSI effects. The implemented algorithm was verified against canonical test cases, addressing the case of a single SDOF structure, linear-elastic Vs non-linear and with/without soil-foundation-structure interaction, over rigid half-space. For all cases, an excellent match with solutions coming from independent numerical codes was found.

In next future, we envisage the following as main further developments on this topic:

- Validate the implemented approach also against available experimental data (e.g. CAMUS IV structure, Combescure et al., 2000);
- Extend the library of structural models included in the current version of SPEED-SCI by including the case of MDOF structures to represent more realistically the seismic response of multi-storey buildings;
- Application to a realistic case study, such as the urban area of Wellington (New Zealand), to investigate and quantify the impact of SCI effects induced by clusters of high-rise buildings. This kind of study may have implications also for the re-insurance industry sector.

6. References

Bradley, B., Tarbali, K., Lee, RL., Huang, J., Motha, J., Bae, S.E., Polak, V., Zhu, M., Schill, C., Patterson, J., Lagrava, D., 2020. Cybershake NZ v19.5: New Zealand simulation-based probabilistic seismic hazard analysis, Proc. of the 2020 New Zealand Society for Earthquake Engineering Annual Technical Conference, Wellington, New Zealand.

Boutin, C., Soubestre, J., Schwan, L., Dietz, M., 2014. Multi-scale modeling for dynamics of structure-soil-structure interactions. Acta Geophys. 62, 1005–1024. https://doi.org/10.2478/s11600-014-0230-9

Combescure, D., Chaudat, T., 2000. ICONS European program seismic tests on R/C walls with uplift; CAMUS IV specimen. ICONS Project, CEA/DRN/DMT Report SEMT/EMSI/RT/00-27/4.

Erlingsson, S., Bodare, A., 1996. Live load induced vibrations in Ullevi Stadium — dynamic dynamic soil analysis. Soil Dyn. Earthq. Eng. 15, 171–188. https://doi.org/10.1016/0267-7261(95)00041-0

Gazetas, G., 1991. Foundation Vibrations, in: Fang, H.-Y. (Ed.), Foundation Engineering Handbook. Springer US, Boston, MA, pp. 553–593. https://doi.org/10.1007/978-1-4615-3928-5_15

Graves, R., Jordan, T.H., Callaghan, S., Deelman, E., Field, E., Juve, G., Kesselman, C., Maechling, P., Mehta, G., Milner, K., Okaya, D., Small, P., Vahi, K., 2011. CyberShake: A Physics-Based Seismic Hazard Model for Southern California. Pure Appl. Geophys. 168, 367–381. https://doi.org/10.1007/s00024-010-0161-6

Graves, R., Pitarka, A., 2016. Kinematic Ground-Motion Simulations on Rough Faults Including Effects of 3D Stochastic Velocity Perturbations. Bull. Seismol. Soc. Am. 106, 2136–2153. https://doi.org/10.1785/0120160088

Gueguen, P., 2000. Experimental and Numerical Analysis of Soil Motions Caused by Free Vibrations of a Building Model. Bull. Seismol. Soc. Am. 90, 1464–1479. https://doi.org/10.1785/0119990072

Guidotti, R., Stupazzini, M., Smerzini, C., Paolucci, R., Ramieri, P., 2011. Numerical Study on the Role of Basin Geometry and Kinematic Seismic Source in 3D Ground Motion Simulation of the 22 February 2011 Mw 6.2 Christchurch Earthquake. Seismol. Res. Lett. 82, 767–782. https://doi.org/10.1785/gssrl.82.6.767

Hans, S., Boutin, C., Ibraim, E., Roussillon, P., 2005. In situ experiments and seismic analysis of existing buildings. Part I: experimental investigations. Earthq. Eng. Struct. Dyn. 34, 1513–1529. https://doi.org/10.1002/eqe.502

Herlin, A ., 2021. A numerical approach to couple the simulation of earthquake ground motion with models for structural response at city level. Master's Thesis submitted at Politecnico di Milano, Italy.

Irikura, K., Miyake, H., 2011. Recipe for Predicting Strong Ground Motion from Crustal Earthquake Scenarios. Pure Appl. Geophys. 168, 85–104. https://doi.org/10.1007/s00024-010-0150-9

Isbiliroglu, Y., Taborda, R., Bielak, J., 2015. Coupled Soil-Structure Interaction Effects of Building Clusters during Earthquakes. Earthq. Spectra 31, 463–500. https://doi.org/10.1193/102412EQS315M

Jennings, P.C., 1970. Distant motions from a building vibration test. Bull. Seismol. Soc. Am. 60, 2037–2043.

Kham, M., Semblat, J.-F., Bard, P.-Y., Dangla, P., 2006. Seismic Site-City Interaction: Main Governing Phenomena through Simplified Numerical Models. Bull. Seismol. Soc. Am. 96, 1934–1951. https://doi.org/10.1785/0120050143

Koketsu, K., Miyake, H., Suzuki, H., 2012. Japan integrated velocity structure model version 1, Proceedings of the 15th World Conference on Earthquake Engineering, (1773).

Komatitsch, D., Tromp, J., 2002. Spectral-element simulations of global seismic wave propagation-I. Validation. Geophys. J. Int. 149, 390–412. https://doi.org/10.1046/j.1365-246X.2002.01653.x

Komatitsch, D., Vilotte, J.-P., 1998. The spectral element method: An efficient tool to simulate the seismic response of 2D and 3D geological structures. Bull. Seismol. Soc. Am. 88, 368–392. https://doi.org/10.1785/BSSA0880020368

Lu, X., McKenna, F., Cheng, Q., Xu, Z., Zeng, X., Mahin, S.A., 2020. An open-source framework for regional earthquake loss estimation using the city-scale nonlinear time history analysis. Earthq. Spectra 36, 806–831. https://doi.org/10.1177/8755293019891724

Martin Mai, P., Beroza, G.C., 2003. A hybrid method for calculating near-source, broadband seismograms: application to strong motion prediction. Phys. Earth Planet. Inter., The quantitative prediction of strong-motion and the physics of earthquake sources 137, 183–199. https://doi.org/10.1016/S0031-9201(03)00014-1

Mazzieri, I., Stupazzini, M., Guidotti, R., Smerzini, C., 2013. SPEED: SPectral Elements in Elastodynamics with Discontinuous Galerkin: a non-conforming approach for 3D multi-scale problems. Int. J. Numer. Methods Eng. 95, 991–1010. https://doi.org/10.1002/nme.4532

McCallen, D., Petersson, A., Rodgers, A., Pitarka, A., Miah, M., Petrone, F., Sjogreen, B., Abrahamson, N., Tang, H., 2021. EQSIM—A multidisciplinary framework for fault-to-structure earthquake simulations on exascale computers part I: Computational models and workflow. Earthq. Spectra 37, 707–735. https://doi.org/10.1177/8755293020970982

Oliveira, S.P., Seriani, G., 2011. Effect of Element Distortion on the Numerical Dispersion of Spectral Element Methods. Commun. Comput. Phys. 9, 937–958. https://doi.org/10.4208/cicp.071109.080710a

Oral, E., Gélis, C., Bonilla, L.F., Delavaud, E., 2017. Spectral element modelling of seismic wave propagation in visco-elastoplastic media including excess-pore pressure development. Geophys. J. Int. 211, 1494–1508. https://doi.org/10.1093/gji/ggx375

Paolucci, R., 1997. SIMPLIFIED EVALUATION OF EARTHQUAKE-INDUCED PERMANENT DISPLACEMENTS OF SHALLOW FOUNDATIONS. J. Earthq. Eng. 1, 563–579. https://doi.org/10.1080/13632469708962378

Paolucci, R., Mazzieri, I., Piunno, G., Smerzini, C., Vanini, M., Özcebe, A.G., 2021. Earthquake ground motion modeling of induced seismicity in the Groningen gas field. Earthq. Eng. Struct. Dyn. 50, 135–154. https://doi.org/10.1002/eqe.3367

Paolucci, R., Mazzieri, I., Smerzini, C., 2015. Anatomy of strong ground motion: near-source records and three-dimensional physics-based numerical simulations of the Mw 6.0 2012 May 29 Po Plain earthquake, Italy. Geophys. J. Int. 203, 2001–2020. https://doi.org/10.1093/gji/ggv405

Rodgers, A.J., Pitarka, A., Pankajakshan, R., Sjögreen, B., Petersson, N.A., 2020. Regional-Scale 3D Ground-Motion Simulations of Mw 7 Earthquakes on the Hayward Fault, Northern California Resolving Frequencies 0–10 Hz and Including Site-Response Corrections. Bull. Seismol. Soc. Am. 110, 2862–2881. https://doi.org/10.1785/0120200147

Sangaraju, S., R. Paolucci., C. Smerzini., 2014. 3D physics-based ground motion simulation of the 2016 Kumamoto earthquakes, Proceedings of the 6th IASPEI/IAEE International Symposium: The Effects of Surface Geology on Seismic Motion (ESG6), Kyoto, Japan, August 2021.

Schiappapietra, E., Smerzini, C., 2021. Spatial correlation of broadband earthquake ground motion in Norcia (Central Italy) from physics-based simulations. Bull. Earthq. Eng. 19, 4693–4717. https://doi.org/10.1007/s10518-021-01160-7

Schwan, L., Boutin, C., Padrón, L.A., Dietz, M.S., Bard, P.-Y., Taylor, C., 2016. Site-city interaction: theoretical, numerical and experimental crossed-analysis. Geophys. J. Int. 205, 1006–1031. https://doi.org/10.1093/gji/ggw049

Semblat, J.-F., Kham, M., Bard, P.-Y., 2008. Seismic-Wave Propagation in Alluvial Basins and Influence of Site-City Interaction. Bull. Seismol. Soc. Am. 98, 2665–2678. https://doi.org/10.1785/0120080093

Sjögreen, B., Petersson, N.A., 2012. A Fourth Order Accurate Finite Difference Scheme for the Elastic Wave Equation in Second Order Formulation. J. Sci. Comput. 52, 17–48. https://doi.org/10.1007/s10915-011-9531-1

Small, P., Gill, D., Maechling, P.J., Taborda, R., Callaghan, S., Jordan, T.H., Olsen, K.B., Ely, G.P., Goulet, C., 2017. The SCEC Unified Community Velocity Model Software Framework. Seismol. Res. Lett. 88, 1539–1552. https://doi.org/10.1785/0220170082

Smerzini, C., Pitilakis, K., Hashemi, K., 2017. Evaluation of earthquake ground motion and site effects in the Thessaloniki urban area by 3D finite-fault numerical simulations. Bull. Earthq. Eng. 15, 787–812. https://doi.org/10.1007/s10518-016-9977-5

Stupazzini, M., Infantino, M., Allmann, A., Paolucci, R., 2021. Physics-based probabilistic seismic hazard and loss assessment in large urban areas: A simplified application to Istanbul. Earthq. Eng. Struct. Dyn. 50, 99–115. https://doi.org/10.1002/eqe.3365

Taborda, R., Bielak, J., 2011. Large-Scale Earthquake Simulation: Computational Seismology and Complex Engineering Systems. Comput. Sci. Eng. 13, 14–27. https://doi.org/10.1109/MCSE.2011.19

Thomson, E.M., Bradley, B.A., Lee, R.L., 2020. Methodology and computational implementation of a New Zealand Velocity Model (NZVM2.0) for broadband ground motion simulation. N. Z. J. Geol. Geophys. 63, 110–127. https://doi.org/10.1080/00288306.2019.1636830

Wirgin, A., Bard, P.-Y., 1996. Effects of buildings on the duration and amplitude of ground motion in Mexico City. Bull. Seismol. Soc. Am. 86, 914–920.

Wolf, J.P., 1985. Dynamic soil-structure interaction, Prentice-Hall international series in civil engineering and engineering mechanics. Prentice-Hall, Englewood Cliffs, N. J.

APPENDIX (USER GUIDE)

1 Introduction

The following user guide is to explain the use of the new version of SPEED (http://speed.mox.polimi.it/), including a module which implements the structural response through simplified structural models and the interaction effects between soil and structures both in presence of a single structure and in presence of multiple structures.

2 Modifications to SPEED code

The use is the same of SPEED, with some differences introduced by the presence of thenew module. New functions added in SPEED program (in alphabetical order):

- **CENTRAL_DIFFERENCE.f90**: solves the equation of motion for the single degree-of-freedom (SDOF) model by means of the central difference scheme
- **COMPUTE _SDOF _INPUT.f90**: computes acceleration and displacement at the base of the structure
- **LINEAR _ELASTIC.f90**: linear elastic (LE) constitutive law for the SDOF model (defines the force from the structural displacement)
- **MAKE SDOF OUTPUT FILES.f90**: creates output files to save the structural motion (explained in detail in the following)
- **MAKE_SDOF_SYSTEM.f90**: reads the properties of the structure from input file *SDOFINFO.txt*
- **PERFECTLY _PLASTIC.f90**: elastoplastic (EPP) constitutive law for the SDOF model (defines the force from the structural displacement)
- **READ_FILESYS.f90**: reads file *SYS.input*, with the position of the structures
- **READ_SDOF_INPUT_FILES.f90**: reads structural properties from input files, together with **MAKE_SDOF_SYSTEM.f90**
- **READ_SYSTEM_POSITION.f90**: reads structure position (this function is called by **SPEED.f90**)
- **SDOF SFS MODEL.f90**: computes response of the four degrees-of-freedom (4DOFs) model
- **SDOF_SHEAR_MODEL.f90**: computes response of the SDOF model
- **TRILINEAR.f90**: trilinear constitutive law for the SDOF model (defines the force from the structural displacement)
- **WRITE_SDOF_OUTPUT_FILES.f90**: writes output files with structural motion (explained in detail in the following)

3 Pre-processing routines

Some MATLAB pre-processing routines, contained in the folder PRE PROC, are used to define the structural properties and generate the files that are necessary for the simula-tions:

- **sdofinput.m**: asks for structure parameters through an interactive interface
- **createSDOFINFO.m**: generates *SDOFINFO.txt* with structural properties, read by **READ_SDOF_INPUT_FILES.f90** and **MAKE_SDOF_SYSTEM.f90**
- **createSYS.m**: generates *SYS.input*, where the structures positions are saved and which is read by **READ_SYSTEM_POSITION.f90**

SDOFINFO.txt

The file containing the structural properties can be found in the folder SDOF _INFO. The structural parameters depend on the type of structural model chosen. In case of the 4DOFs oscillator the values of parameters β and γ used by the Newmark's method for solving the structural equilibrium equation are also provided.
The file format is the following:

Number of structures
Structure ID, Constitutive law (1- Linear elastic, 2- Elastoplastic, 3- Trilinear)
Structural model (0- SDOF, 1- 4DOFs, only in case of LE oscillator) Structure parameters
Newmark method coefficients β and γ (only in case of the 4DOFs model)
...
Structure ID, Constitutive lawStructural model
Structure parameters
β and γ

Depending on the chosen structural model, the structural parameters are displayed asfollows:

- LE SDOF model parameters: mass, stiffness, damping factor, natural period
- EPP SDOF model parameters: mass, stiffness, damping factor, yield strength, natural period
- trilinear SDOF model: mass, stiffness, hardening coefficient, softening coefficient, damping factor, yield strength, peak displacement, ultimate displacement, natural period
- 4DOFs model: superstructure mass, foundation mass, sum of centroidal moment of inertia, height, superstructure stiffness, foundation equivalent spring coefficient associated to horizontal, rocking and vertical DOF, superstructure damping factor, foundation equivalent dashpot coefficient associated to horizontal, rocking and vertical DOF, superstructure natural period

SYS.input

The file contains the position of the structure(s) in the following format :

———————

Number of structures
Structure ID, Structure coordinates (x, y, z)
...
Structure ID, Structure coordinates (x, y, z)

———————

Other modifications have been added to the original input files:

SPEED.input

Aside from the original parameters, the following new keywords are included:

- **SDOFFILE** FILENAME

FILENAME defines the folder where the input file *SDOFINFO.txt* is found.

- **SDOFOUT** DIS ACC FOR

DIS ACC and FOR are assigned value 1 or 0 if the values of displacement, acceler-ation and force have to be saved in the correspondent files.

- **SYSLST** DEPTH VAL

DEPTH defines the starting depth from which the oscillator position should be searched, VAL assumes value 1 or 0 if the file *SLST.input* should be read or written in the working directory.

Site.mate

This file originally contains information on the soil characteristics in all different regionsof the domain and on the external loads and boundary conditions. Some additional parameters have been added, which coincide with two new function types and a new keyword.

- **FUNC** NF 773 PARAMETERS

With this new function type, the external loading values defined at each time in- stant are read from a given file. The required parameters are the number of valuescontained in the file and the file name.

- **FUNC** NF 777 PARAMETERS

This function type defines a concentrated load to be added as boundary excitationto the soil domain. It is used to simulate the interaction between structure and soil. The dummy parameters are assigned as 1 1 1.

- **PLOD** NF VAL BID

This command defines a concentrated load of amplitude scaled by VAL to be as- signed to the point where the oscillator BID is positioned in order to account for the exchange of soil-structure interaction force. NF must match the value of NF given for the function type 777.

We point out that the name of the files *Site.mate* and *Site.mesh* can be chosen by theuser, but must be specified in *SPEED.input*.
A description of the functioning of the MATLAB pre-processing routines is provided in

the Figure 17.

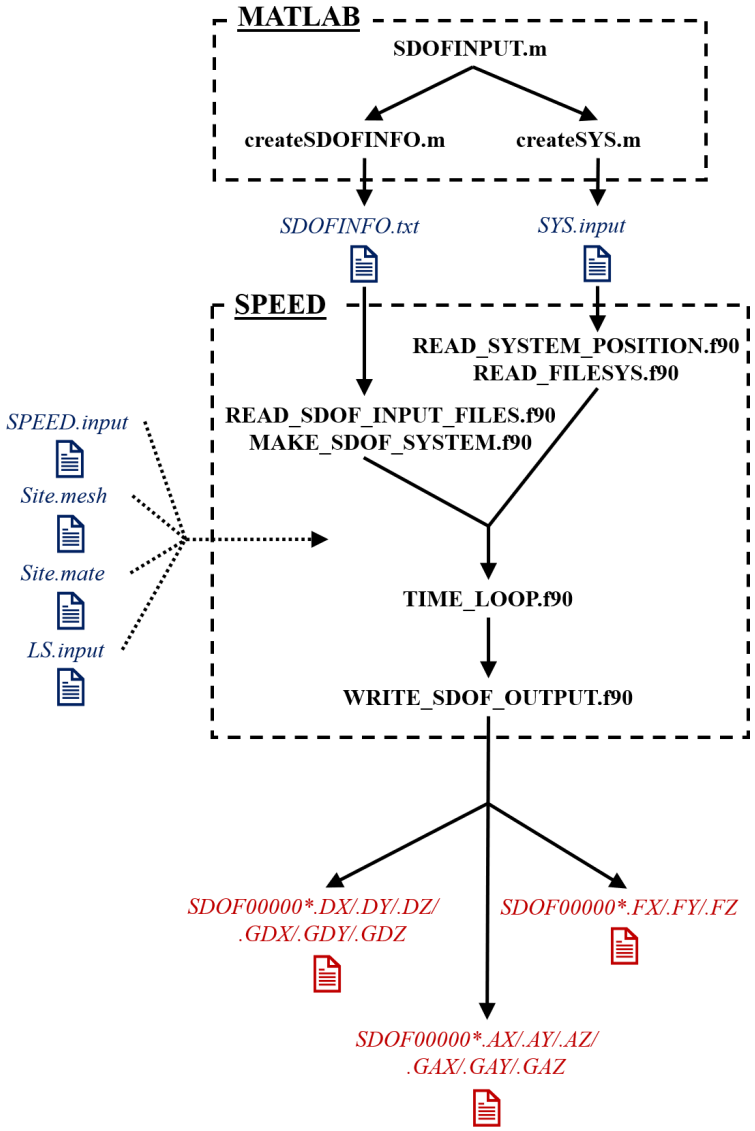

Figure 17 Input-output workflow of simulation.

4 Post-processing routines

Finally, the following MATLAB post-processing routines, contained in the folder POST_PROC, are used to analyse the structural response saved in the output files which havebeen generated by **WRITE SDOF OUTPUT FILES.f90**

- **REWRITE_MONITOR_FORMAT.m**: rewrites output files in new format
- **PLOT_MONITORS.m**: generates plots of structural response and soil motion captured by the receivers
- **SOIL_Ampl_function.m**: computes the soil transfer function in correspondence of the ground surface

- **FourierTransform.m**: computes the Fourier transform of a given input
- **SDOF_Ampl_function**: computes the structural transfer function

4.1 The output files

We provide here a description of all output files generated by **WRITE SDOF OUTPUT - FILES.f90** containing the structural response. Different files are written, depending on the type of structural model chosen for the building (SDOF or 4DOFs) and on the val- ues given to the variable SDOFOUT in *SPEED.input*, whose role is explained previously.
They`ıse files are saved in the folder MONITORS, where the soil motion files are alsosaved.

- SDOF structural model
  - *SDOF000000.DX/DY/DZ* contains the structural displacement in the three directions x, y and z
  - *SDOF000000.GDX/GDY/GDZ* contains the soil displacement at the base of the structure in the three directions x, y and z
  - *SDOF000000.AX/AY/AZ* contains the structural acceleration in the three directions x, y and z
  - *SDOF000000.GAX/GAY/GAZ* contains the soil acceleration at the base of the structure in the three directions x, y and z
  - *SDOF000000.FX/FY/FZ* contains the structural interaction force in the three directions x, y and z
- 4DOFs structural model
  - *STR000000.DX/DY* contains the structural displacement in directions x and y
  - *GRD000000.DX/DY/DZ* contains the soil displacement at the base of the structure in the three directions x, y and z
  - *FND000000.DX/DY* contains the foundation displacement in directions x and y
  - *FND000000.DRX/DRY* contains the foundation rotation which produces structural displacement in directions x and y, respectively
  - *FND000000.DZX/DZY* contains the structural displacement in direction z associated to the structural main degree-of-freedom (along direction x or y)
  - *STR000000.AX/AY* contains the structural acceleration in directions x and y
  - *GRD000000.AX/AY/AZ* contains the soil acceleration at the base of the structure in the three directions x, y and z
  - *FND000000.AX/AY* contains the foundation acceleration in directions x and y
  - *FND000000.DAX/DAY* contains the foundation rocking acceleration which produces structural acceleration in directions x and y, respectively
  - *FND000000.AZX/AZY* contains the structural acceleration in direction z associated to the structural main degree-of-freedom (along direction x or y)
  - *STR000000.FX/FY* shear force developed by the superstructure

– *FND000000.FX/FY* shear force developed by the foundation
– *INT000000.FX/FY/FZ* interaction force between foundation and soil